We are IntechOpen,
the world's leading publisher of
Open Access books
Built by scientists, for scientists

5,100
Open access books available

127,000
International authors and editors

145M
Downloads

Our authors are among the

154
Countries delivered to

TOP 1%
most cited scientists

12.2%
Contributors from top 500 universities

CLARIVATE ANALYTICS
BOOK CITATION INDEX
INDEXED

WEB OF SCIENCE™

Selection of our books indexed in the Book Citation Index
in Web of Science™ Core Collection (BKCI)

Interested in publishing with us?
Contact book.department@intechopen.com

Numbers displayed above are based on latest data collected.
For more information visit www.intechopen.com

Control Mechanisms of Energy Storage Devices

Mahmoud Elsisi

Abstract

The fast acting due to the salient features of energy storage systems leads to using of it in the control applications in power system. The energy storage systems such as superconducting magnetic energy storage (SMES), capacitive energy storage (CES), and the battery of plug-in hybrid electric vehicle (PHEV) can storage the energy and contribute the active power and reactive power with the power system to extinguish the rapid change in load demands and the renewable energy sources (RES). This chapter gives an overview about the modeling of energy storage devices and methods of control in them to adjust steady outputs.

Keywords: energy storage devices, superconducting magnetic energy storage (SMES), capacitive energy storage (CES), plug-in hybrid electric vehicle (PHEV)

1. Introduction

With the increasing of distributed generator (DG) technologies, large numbers of DGs are connected with the grid in different forms, such as wind and solar power systems [1–3]. Because of the fluctuations of their output power, energy storage devices are utilized to adjust steady outputs [4, 5]. In fact, the characteristics of the different storage devices vary widely, including the amount of energy stored and the time for which this stored energy is required to be retained or released [6, 7]. The superconducting magnetic energy storage (SMES), superconducting capacitive energy storage (CES), and the battery of plug-in hybrid electric vehicle (PHEV) are able to achieve the highest possible power densities. Each storage energy device has a different model. Several control approaches are applied to control the energy storage devices. In [8, 9], model predictive control (MPC) is presented for residential energy systems with photovoltaic (PV) system and batteries. Model predictive control predicts the load and the generation over a certain time horizon into the future and finds the optimum schedule of the battery over that period which can minimize a desired objective. In [10], a voltage regulation in distribution feeders is proposed using residential energy storage units. The control method is carried out by making the charging and discharging rates of the batteries a function in the voltage at the point of common coupling. A fuzzy logic based control method of battery state of charge (SOC) is presented in [11]. This control method regulates the battery SOC at expected conditions, and consequently the energy capacity of BESS can be small. In [12], a state-of-charge feedback control technique is used to keep the charging level of the battery within its proper range while the battery energy storage system make the output fluctuation of a wind farm smooth. The optimal

design of MPC with SMES based on the bat-inspired algorithm (BIA) is introduced for load frequency control in [13]. This work is extended to include the MPC with SMES and CES in [14]. Decentralized MPC with PHEVs is utilized for frequency regulation in a smart three-area interconnected power system in [15].

2. Superconducting magnetic energy storage

The SMES units are used to compensate the load increments by the injection of a real power to the system and diminished the load decrements by the absorbing of the excess real power via large superconducting inductor [16–18]. **Figure 1a** show a schematic diagram of SMES unit consists of superconducting inductor (L), Y-Y/Δ transformer, and controlled ac/dc bridge converter with 12-pulse thyristor. A power conversion system (PCS) is used to connect the superconducting inductor with the AC grid. The PCS is a dual-mode converter and it works as a rectifier or as an inverter in the charging and discharging modes of the inductor respectively. Obviously, the mode of operation is detected according to the nature of load perturbation. The charging phase represents the rectifier mode. In the rectifier mode, adjusted positive voltage is applied across the terminals of the inductor. Alternatively, the discharging phase represents the inverter mode. In the inverter mode, adjusted negative voltage is applied across the terminals of the inductor. The controlling in the thyristor firing angle is used to switch either rectifier or inverter modes, the converter output voltage is expressed in kV and it is given in following equation [19]:
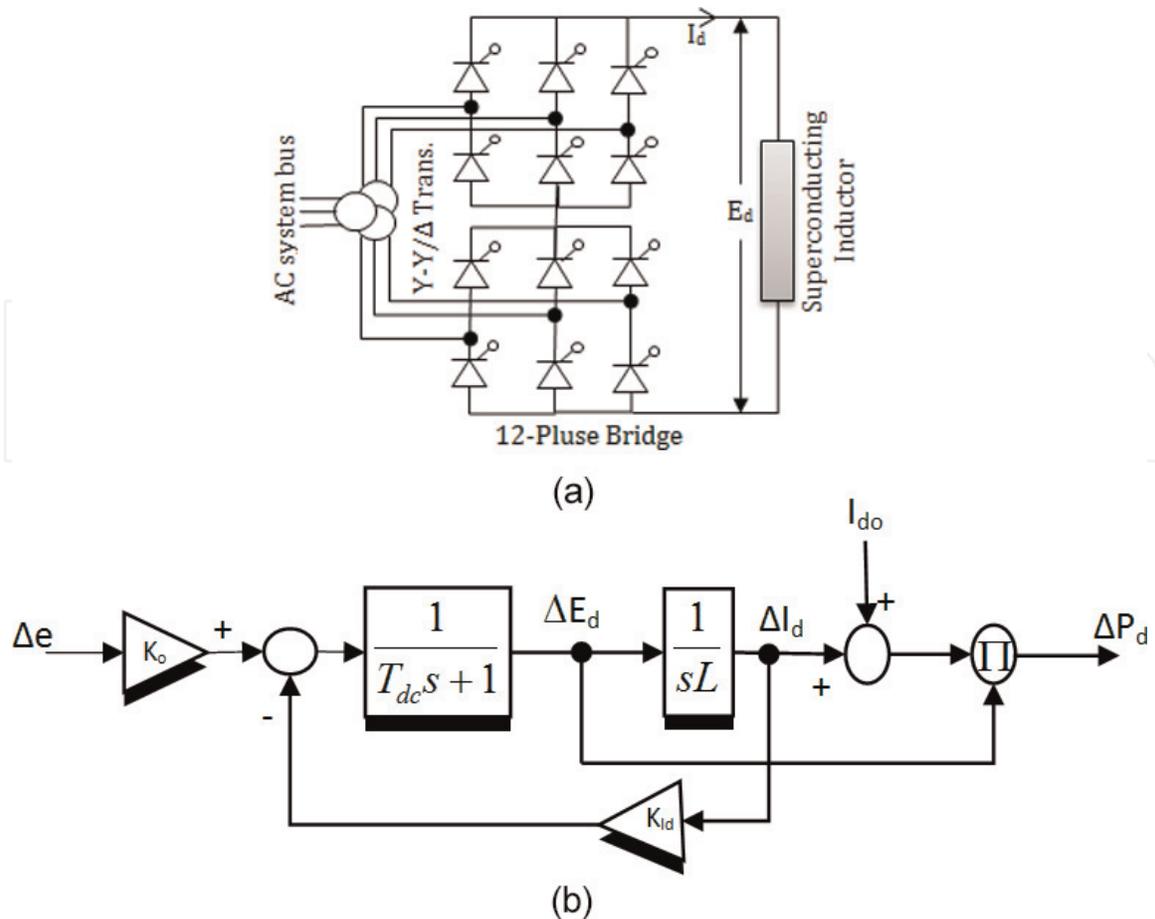
$$E_d = 2E_o \cos(\alpha) - 2I_d R_c \tag{1}$$

Figure 1.
The SMES unit (a) circuit diagram and (b) corresponding block diagram.

where E_d is the inductor DC voltage (kV); E_o is the converter open circuit voltage (kV); α is the thyristor firing angle (degrees); I_d is the inductor current (kA); R_C is the equivalent resistance of commutation (ohm).

2.1 Modeling of superconducting magnetic energy storage

According to the rectifier or inverter modes, the polarity of the voltage E_d is adjusted while the direction of inductor current I_d does not change. As mention in the above section, the regulation of the thyristor firing angle is used to controlling the direction and magnitude of the inductor power P_d. Initially, a small positive voltage is applied to charge the inductor to its rated current according to the desired charging period of the SMES unit. The inductor voltage is reduced to zero and the inductor current reach to its rated value because the coil is superconducting. When the inductor current reached to its rated value, the SMES unit can be coupled to the power system. The error signal Δe represent the input to control the SMES voltage E_d. This error signal may be the change of system frequency, the change of system voltage, or the change of system current according to the control object. The incremental voltage and current changes of the SMES coil are given as follows:

$$\Delta E_d = \frac{K_o}{1 + sT_{dc}}(\Delta e) \tag{2}$$

$$\Delta I_d = \frac{1}{sL}\Delta E_d \tag{3}$$

where T_{dc} is the converter time constant in sec, K_o is the gain of the proportional controller in kV/Hz and s is the Laplace operator. As reported in [19], the inductor current reaches to its nominal value very slowly in the SMES unit. So, the fast rate of the current to restore its rated value is required to extinguish the next load perturbation fastly. Therefore, a negative feedback signal is used in the SMES control loop to provide fast current recovery. Thus, Eq. 2 is rewritten in following form:

$$\Delta E_d = \frac{1}{1 + sT_{dc}}(K_o \Delta e - K_{Id}\Delta I_d) \tag{4}$$

where K_{Id} is the negative feedback gain of the current deviation (kV/kA). In the storage mode, the coil is short-circuited, i.e. $E_{do} = 0$ and there is no power transfer. So in either phase (charging/discharging), the power is defined by $P_d = E_d I_d$ and the initial inductor power is $P_{do} = E_{do}I_{do}$, where E_{do} and I_{do} are the voltage and current magnitudes previous to load disturbance. The inductor power following to the load disturbance is defined as follows:

$$\begin{aligned} P_d &= (E_{do} + \Delta E_d)(I_{do} + \Delta I_d) \\ &= E_{do}I_{do} + E_{do}\Delta I_d + I_{do}\Delta E_d + \Delta E_d \Delta I_d = P_{do} + E_{do}\Delta I_d + I_{do}\Delta E_d + \Delta E_d \Delta I_d, \ E_{do} = 0 \end{aligned} \tag{5}$$

Therefore, the real power incremental change ΔP_d of the SMES unit in MW is computed as follows:

$$\Delta P_d = P_d - P_{do} = I_{do}\Delta E_d + \Delta I_d \Delta E_d \tag{6}$$

The corresponding block diagram of an SMES incorporating the negative feedback of the current deviation is shown in **Figure 1b**.
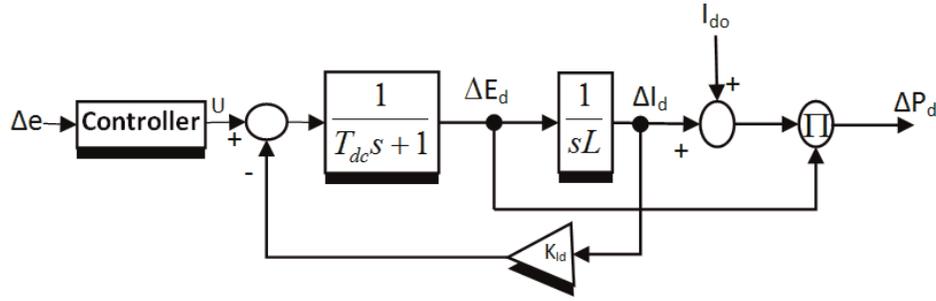
Figure 2.
The block diagram of SMES with controller.

Setting the parameters (L, K_o, K_{Id} and I_{do}) of the SMES unit to their optimistic values can enhance its role in achieving well-damped to the responses. Herein, the application of artificial intelligence (AI) techniques is suggested to search for the optimal parameters of the SMES and controller simultaneously.

2.2 Control techniques of SMES

Modern control techniques such as adaptive control, fuzzy logic control, and model predictive control (MPC) can be applied to control the charging and discharging of the SMES instead of the proportional controller as shown in **Figure 2**. The controller and SMES parameters must be adjusted by proper optimization technique such as genetic algorithm (GA), particle swarm optimization (PSO), and artificial bee colony (ABC),...etc. to give a good performance.

3. Capacitive energy storage

The capacitive energy storage (CES) has an important role to stabilize the power system against to the sudden change in load demand. The static operation of the CES makes its response faster than of the mechanical systems [20–23]. Parallel storage capacitors form the CES. **Figure 3a** shows a schematic diagram of a CES unit connected with the AC grid by a PCS. The capacitor bank dielectric and leakage losses are defined by the resistance (R). When the load demand decreases, the capacitor charges up to its rated full value, thus releases an amount of the excess energy in the system. Contrary, the capacitor discharges to its initial value of voltage when the load demand rises suddenly and release the stored energy fastly to the grid through the PCS. A gate turn-off (GTO) thyristors is used as switches to control the direction of the capacitor current during the charging and discharging as shown in **Table 1**.

The controlling in the thyristor firing angle is used to switch either rectifier or inverter modes of CES to adjust the capacitor voltage as defined in Eq. 1.

3.1 Modeling of superconducting magnetic energy storage

The CES unit is ready to be coupled to the power system for LFC when the rated voltage across the capacitor is attained. The current I_d of CES is controlled by sensing the error signal Δe. This error signal may be the change of system frequency, the change of system voltage, or the change of system current according to the control object. The incremental current changes of the CES are given as follows:

$$\Delta I_d = \frac{K_c}{1 + sT_{dc}} (\Delta e) \qquad (7)$$

where K_c is the proportional controller in kA/Hz.

As stated in [20], the CES voltage reaches to its nominal value very slowly. So, the fast rate of the capacitor voltage to restore its rated value is required to extinguish the next load perturbation fastly. Therefore, a negative feedback signal is used in the CES control loop to provide a fast voltage recovery. Thus, Eq. 7 is rewritten in following form:

$$\Delta I_d = \frac{1}{1 + sT_{dc}} (K_c \Delta f - K_{Ed} \Delta E_d) \qquad (8)$$

where K_{Ed} is the negative feedback gain of the capacitor voltage deviation (kA/kV). In the storage mode, the capacitor represents an open circuit, i.e. $I_{do} = 0$
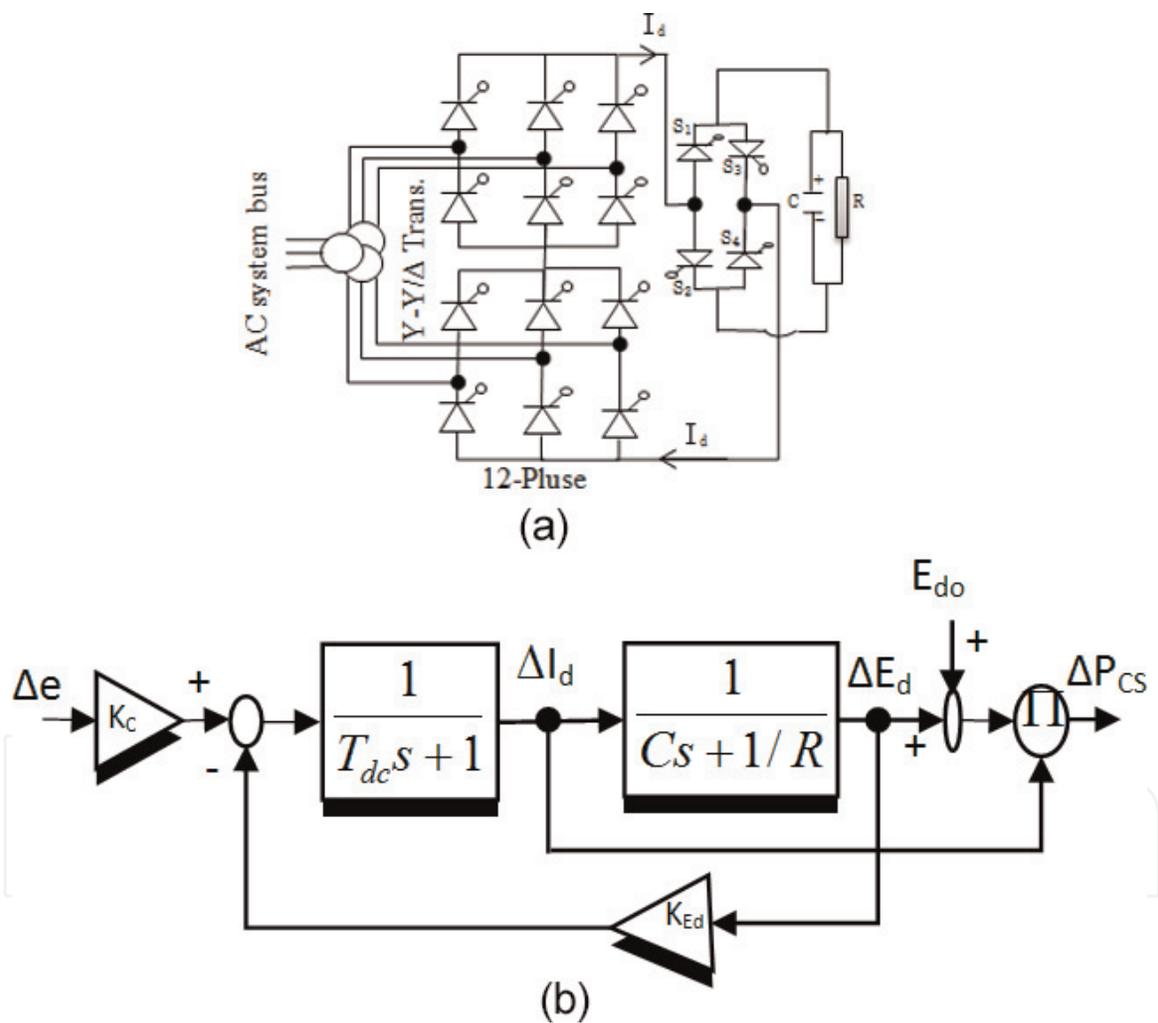

Figure 3.
The CES unit (a) circuit diagram and (b) corresponding block diagram.

	Charging mode	Discharging mode
S₁, S₄	ON	OFF
S₂, S₃	OFF	ON

Table 1.
The modes of switches during the charging and discharging of CES unit.
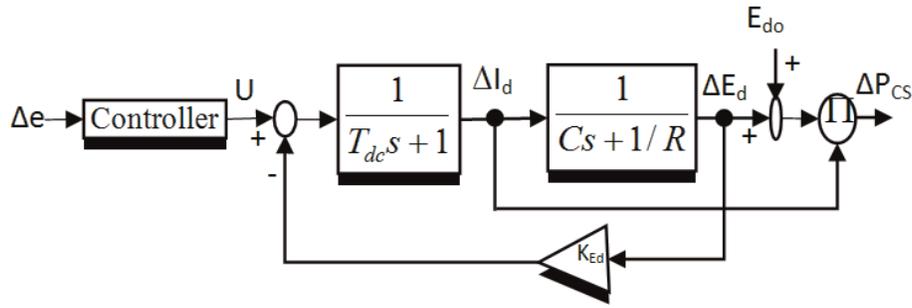
Figure 4.
The block diagram of CES with controller.

and no power transfer. Hence, the power is defined by $P_{CS} = E_d I_d$ and the initial CES power is $P_{CSo} = E_{do} I_{do}$, where E_{do} and I_{do} are the magnitudes of the voltage and current prior to load disturbance. Following a load disturbance, the power flow into the CES is given as follows:

$$P_{CS} = (E_{do} + \Delta E_d)(I_{do} + \Delta I_d)$$
$$= E_{do}I_{do} + E_{do}\Delta I_d + I_{do}\Delta E_d + \Delta E_d\Delta I_d = P_{CSo} + E_{do}\Delta I_d + I_{do}\Delta E_d + \Delta E_d\Delta I_d, \ I_{do} = 0$$

$$(9)$$

Thus, the real power incremental change ΔP_{CS} of the CES unit in MW is computed as follows:

$$\Delta P_{CS} = P_{CS} - P_{CSo} = E_{do}\Delta I_d + \Delta E_d\Delta I_d \qquad (10)$$

The corresponding block diagram of a CES unit incorporating the negative feedback of the voltage deviation is shown in **Figure 3b**.

Setting the parameters (C, K_c, K_{Ed} and E_{do}) of the CES unit to their optimistic values can enhance its role in achieving well-damped to the responses. Herein, the application of artificial intelligence (AI) techniques is suggested to search for the optimal parameters of the CES and controller simultaneously.

3.2 Control techniques of CES

Modern control techniques such as adaptive control, fuzzy logic control, and MPC can be applied to control the charging and discharging of the CES instead of the proportional controller as shown in **Figure 4**. The controller and CES parameters must be adjusted by proper optimization technique such as GA, PSO, and ABC, …etc. to give a good performance.

4. Plug-in hybrid electric vehicle model

The PHEV model is represented as first-order transfers function with very small time constant T_{PHEV} as shown in **Figure 5(a)** [24–27]. The change of PHEV output power ΔP_{PHEV} for charging or discharging is selected according to the control signal U_i of the controller. In this chapter, the control signal is determined by modern control techniques such as adaptive control, fuzzy logic control, and model predictive control (MPC). The control signal depends on the error signal to adjust the charging or discharging of PHEVs batteries. **Figure 5(b)** shows a bi-directional PHEV to charging and discharging power control 'vehicle to grid (V2G)'. According to the change of error, this V2G release a power to the grid or drain power from the
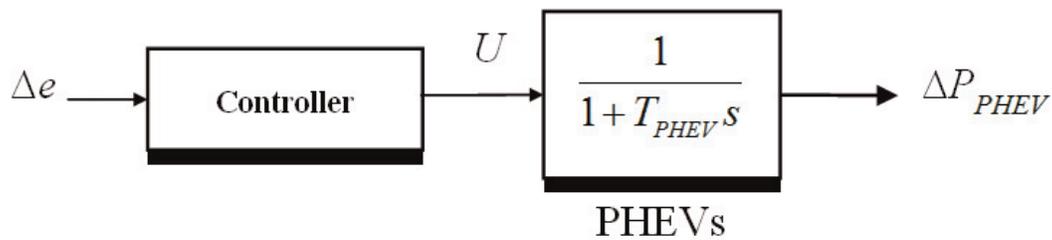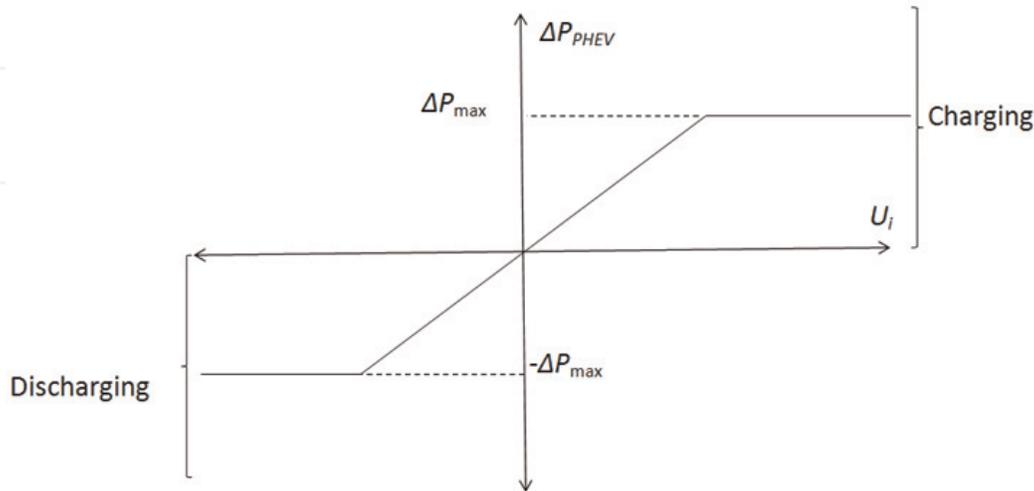
Figure 5.
PHEV model: (a) PHEV with controller block diagram, (b) change of PHEV output power against control signal.

grid. The change of PHEV output power is adjusted by the control signal (U) according to the limit range of output power deviation of PHEV as

$$\Delta P_{PHEV} = \begin{cases} U_i, \ |U_i| \leq \Delta P_{max} \\ \Delta P_{max}, \ U_i > \Delta P_{max} \\ -\Delta P_{max}, \ U_i < -\Delta P_{max} \end{cases} \quad (11)$$

where P_{max} is the maximum PHEV power.

5. Conclusion

In this chapter, classifications of energy storage devices and control strategy for storage devices by adjusting the performance of different devices and features of the power imbalance are presented. The modeling of each storage energy devices is discussed. Furthermore, the control method for each one are cleared. These energy storage devices with modern control techniques such as adaptive control, fuzzy logic control, and model predictive control (MPC) can be applied to extinguish the rapid change in load demands and the fluctuations of RES.

Author details

Mahmoud Elsisi
Electrical Power and Machines Department, Faculty of Engineering (Shoubra),
Benha University, Cairo, Egypt

*Address all correspondence to: mahmoud.elsesy@feng.bu.edu.eg

IntechOpen

References

[1] Heide D, Greiner M, Von Bremen L, Hoffmann C. Reduced storage and balancing needs in a fully renewable European power system with excess wind and solar power generation. Renewable Energy. 2011;**36**(9): 2515-2523

[2] Yamegueu D, Azoumah Y, Py X, Kottin H. Experimental analysis of a solar PV/diesel hybrid system without storage: Focus on its dynamic behavior. International Journal of Electrical Power & Energy Systems. 2013;**44**(1):267-274

[3] Datta M, Senjyu T, Yona A, Funabashi T. Frequency control of photovoltaic–diesel hybrid system connecting to isolated power utility by using load estimator and energy storage system. IEEJ Transactions on Electrical and Electronic Engineering. 2010;**5**(6): 677-687

[4] Dıaz-Gonzalez F, Sumper A, Gomis-Bellmunt O, Villafafila-Robles R. A review of energy storage technologies for wind power applications. Renewable and Sustainable Energy Reviews. 2012; **16**(4):2154-2171

[5] Bandara K, Sweet T, Ekanayake J. Photovoltaic applications for offgrid electrification using novel multi-level inverter technology with energy storage. Renewable Energy. 2012;**37**(1):82-88

[6] Zhou Z, Benbouzid M, Fredéric Charpentier J, Scuiller F, Tang T. A review of energy storage technologies for marine current energy systems. Renewable and Sustainable Energy Reviews. 2013;**18**:390-400

[7] Di Fazio A, Erseghe T, Ghiani E, Murroni M, Siano P, Silvestro F. Integration of renewable energy sources, energy storage systems, and electrical vehicles with smart power distribution networks. Journal of

Ambient Intelligence and Humanized Computing. 2013;**4**:663-671

[8] Schreiber M, Hochloff P. Capacity-dependent tariffs and residential energy management for photovoltaic storage systems. In: Power and Energy Society General Meeting (PES), IEEE. 2013. pp. 1-5

[9] Worthmann K, Kellett CM, Braun P, Grüne L, Weller SR. Distributed and decentralized control of residential energy systems incorporating battery storage. IEEE Transactions on Smart Grid. 2015;**6**(4):1914-1923

[10] Wang Y, Wang BF, Son PL. A voltage regulation method using distributed energy storage systems in lv distribution networks. In: Energy Conference (ENERGYCON), IEEE. 2016. pp. 1-6

[11] Li X, Hui D, Wu L, Lai X. Control strategy of battery state of charge for wind/battery hybrid power system. In: IEEE International Symposium on Industrial Electronics (ISIE). 2010. pp. 2723-2726

[12] Yoshimoto K, Nanahara T, Koshimizu G, Uchida Y. New control method for regulating state-of-charge of a battery in hybrid wind power/battery energy storage system. In: Power Systems Conference and Exposition, IEEE PES. 2006. pp. 1244-1251

[13] Elsisi M, Soliman M, Aboelela MAS, Mansour W. Optimal design of model predictive control with superconducting magnetic energy storage for load frequency control of nonlinear hydrothermal power system using bat inspired algorithm. Journal of Energy Storage. 2017;**12**:311-318

[14] Elsisi M, Soliman M, Aboelela MAS, Mansour W. Improving the grid frequency by optimal design of model

predictive control with energy storage devices. Optimal Control Applications and Methods. 2018;**39**(1):263-280

[15] Elsisi M, Soliman M, Aboelela MAS, Mansour W. Model predictive control of plug-in hybrid electric vehicles for frequency regulation in a smart grid. IET Generation, Transmission & Distribution. 2017;**11**(16):3974-3983

[16] Ali MH, Wu B, Dougal RA. An overview of SMES applications in power and energy systems. IEEE Transactions on Sustainable Energy. 2010;**1**(1):38-47

[17] Bhatt P, Roy R, Ghoshal SP. Comparative performance evaluation of SMES–SMES, TCPS–SMES and SSSC–SMES controllers in automatic generation control for a two-area hydro–hydro system. International Journal of Electrical Power & Energy Systems. 2011;**33**(10):1585-1597

[18] Banerjee S, Chatterjee JK, Tripathy SC. Application of magnetic energy storage unit as load-frequency stabilizer. IEEE Transactions on Energy Conversion. 1990;**5**(1):46-51

[19] Tripathy SC, Balasubramanian R, Chandramohanan Nair PS. Adaptive automatic generation control with superconducting magnetic energy storage in power systems. IEEE Transactions on Energy Conversion. 1992;**7**(3):434-441

[20] Tripathy SC. Improved load-frequency control with capacitive energy storage. Energy Conversion and Management. 1997;**38**(6):551-562

[21] Abraham RJ, Das D, Patra A. Automatic generation control of an interconnected power system with capacitive energy storage. International Journal of Electrical Power and Energy Systems Engineering. 2010;**3**(1):351-356

[22] Sanki P, Ray S, Shukla RR, Das D. Effect of different controllers and capacitive energy storage on two area interconnected power system model using Matlab Simulink. In: 2014 First International Conference on Automation, Control, Energy and Systems (ACES). pp. 1-6

[23] Dhundhara S, Verma YP. Evaluation of CES and DFIG unit in AGC of realistic multisource deregulated power system. International Transactions on Electrical Energy Systems. 2016:1-14

[24] Vachirasricirikul S, Ngamroo I. Robust LFC in a smart grid with wind power penetration by coordinated V2G control and frequency controller. IEEE Transactions on Smart Grid. 2014;**5**(1):371-380

[25] Pahasa J, Ngamroo I. PHEVs bidirectional charging/discharging and SoC control for microgrid frequency stabilization using multiple MPC. IEEE Transactions on Smart Grid. 2015;**6**(2):526-533

[26] Pahasa J, Ngamroo I. Coordinated control of wind turbine blade pitch angle and PHEVs using MPCs for load frequency control of microgrid. IEEE Systems Journal. 2016;**10**(1):97-105

[27] Pahasa J, Ngamroo I. Simultaneous control of frequency fluctuation and battery SOC in a smart grid using LFC and EV controllers based on optimal MIMO-MPC. Journal of Electrical Engineering & Technology. 2017;**12**(2):601-611